DIAGNOSTYKA, 2025, Vol. 26, No. 4

e-ISSN 2449-5220
DOI: 10.29354/diag/214634

ULTRASONIC TESTING DATA DENOISING AND IMAGE ENHANCEMENT METHOD COMBINED WITH FUZZY ALGORITHM

Wei SONG [1,*], Huazhen XU [1], Jianlin QIU [2]

[1] School of Yonyou Digital and Intelligence, Nantong Institute of Technology, Nantong 226002, Jiangsu, China
[2] School of Artificial Intelligence and Computer Science, Nantong University, Nantong 226002, Jiangsu, China
* Corresponding author's email: songwei163@hotmail.com

Abstract

This paper proposes an ultrasound data denoising and image enhancement method combining fuzzy logic and genetic algorithm optimization to improve imaging quality and diagnostic accuracy. Ultrasound imaging, widely used in medical and industrial testing, is often degraded by speckle, thermal and quantization noise, reducing clarity and contrast. To address this, a fuzzy system was designed including fuzzification interface, rule base, inference engine, and defuzzification output, with Gaussian membership functions adaptively tuned through genetic algorithms. Experiments were conducted on the Duke Abdominal Ultrasound Dataset and the BUS Breast Ultrasound Dataset, and the results were evaluated using signal-to-noise ratio (SNR), peak signal-to-noise ratio (PSNR), and structural similarity index (SSIM). Compared with mean filter, median filter, wavelet transform, adaptive Wiener filter, and convolutional neural networks, the proposed method achieved consistent improvements. For instance, on abdominal ultrasound images, the fuzzy algorithm increased SNR by approximately 5.5% and PSNR by 6.4% compared with CNN, while SSIM improved by 2.3%. On breast ultrasound data, the method yielded a 5.6% higher SNR, a 5.5% higher PSNR, and a 2.3% higher SSIM than CNN. These results show integrating fuzzy logic and genetic optimization offers an effective, efficient, generalizable ultrasound image enhancement strategy, with potential clinical and industrial use.

Keywords: Ultrasonic testing, data denoising, image enhancement, fuzzy algorithm, signal processing

1. INTRODUCTION

As a non-destructive testing method, ultrasonic testing has been widely applied in fields such as medical diagnosis and industrial inspection. With the advancement of ultrasonic imaging technology, image quality and resolution have continuously improved. However, in practical applications, ultrasonic signals are easily affected by various types of noise, resulting in blurred images or loss of detail, which compromises the accuracy and reliability of test results. Therefore, effectively removing noise and enhancing image quality has become a key research focus [1].

In recent years, with the progress of computer technology and digital signal processing, many advanced denoising and image enhancement algorithms have been proposed and applied to ultrasonic testing [2]. However, traditional methods often struggle to balance noise reduction and detail preservation, especially under complex noise conditions. Fuzzy logic, as a mathematical tool capable of simulating human reasoning, demonstrates strong adaptability in processing uncertain information. By incorporating fuzzy algorithms, new approaches can be developed for denoising and enhancing ultrasonic testing data, which not only improve image clarity but also better preserve useful information in the original images. This study aims to explore data processing methods for ultrasonic testing based on fuzzy algorithms, contributing to improvements in ultrasonic imaging quality.

At present, both domestic and international scholars have conducted extensive research on improving the quality of ultrasonic detection images. Traditional denoising techniques mainly include spatial domain filtering (mean filtering) [3] and frequency domain filtering (Fourier transform) [4]. Although these methods are simple and straightforward, they often lead to issues such as edge blurring. With the rise of machine learning, particularly deep learning, neural network-based models have been introduced into ultrasonic image processing. For example, convolutional neural

Received 2025-02-19; Accepted 2025-11-24; Available online 2025-11-25

networks (CNNs) [5] show strong performance in feature extraction and classification. In addition, advanced signal processing techniques such as wavelet transform and adaptive filtering have also been widely used. While these methods have achieved promising results, they remain limited in handling certain noise types and in preserving overall image structure.

Studies have demonstrated that fuzzy control strategies can significantly improve the quality of ultrasonic images, especially under low-contrast conditions. Nevertheless, designing a suitable fuzzy system architecture and selecting appropriate parameters remain major challenges [6, 7].

This study focuses on enhancing the denoising and image quality of ultrasound data through the integration of fuzzy logic algorithms, aiming to improve imaging quality and diagnostic accuracy. As ultrasound imaging has become an indispensable part of medical examinations, it is often degraded by various types of noise, such as speckle and electronic noise. These issues result in low clarity and low contrast, which can impair clinical judgment and potentially delay treatment. Therefore, this study is dedicated to developing an efficient and reliable processing method that can effectively suppress these interferences, preserve or even enhance useful image information, and provide more accurate data support for clinical applications.

To achieve these objectives, this study first reviews the basic principles of ultrasound detection and its specific applications in medical imaging, and analyzes the causes and characteristics of different noise types. It then examines existing denoising and enhancement techniques, focusing on both traditional signal processing approaches (wavelet transform) and modern machine learning methods (deep neural networks). Building on this foundation, the paper introduces the core concepts of fuzzy set theory and its application in signal processing. A complete fuzzy logic system is subsequently designed for ultrasound image denoising, comprising a fuzzification interface, a rule base, and a defuzzification output module. Several fuzzy operator-based enhancement strategies are also proposed to optimize visual quality while maximizing detail preservation. Finally, the proposed approach is evaluated through a series of quantitative metrics and compared with state-of-the-art algorithms.

This study highlights the originality of applying fuzzy algorithms to ultrasound data denoising and image enhancement by integrating genetic optimization into membership function design. Unlike conventional filtering or deep learning models that often struggle to balance detail preservation and noise reduction, the proposed approach addresses both challenges simultaneously. The significance of this work lies in offering a computationally efficient and generalizable solution that reduces dependency on large datasets while achieving superior quantitative performance. It emphasizes not only technical novelty but also practical importance in clinical diagnostics and industrial testing.

The primary focus is on medical ultrasound imaging, particularly abdominal and breast ultrasound datasets, where image quality directly affects diagnostic accuracy. Although fuzzy algorithms can also be applied in industrial ultrasonic testing for defect detection, such contexts are not analyzed in detail here. Instead, references to industrial usage are retained only for comparison in the theoretical background. This separation ensures that the contributions and experimental validations are clearly positioned within the medical imaging field while acknowledging broader applicability.

2. RELEVANT THEORETICAL BASIS

2.1. Principle of Ultrasonic Testing

Ultrasound is a sound wave with a frequency higher than the human hearing range (usually greater than 20kHz). In medical imaging, ultrasound detection uses the propagation characteristics of ultrasound in different media to perform imaging. When ultrasound is transmitted from one medium to another, reflection, refraction, and scattering occur at the interface. By analyzing these echo signals, an image of the tissue structure can be constructed. The propagation speed v of ultrasound is related to the elastic modulus E and density of the medium ρ, as shown in Formula 1 [8, 9].

$$v = \sqrt{\frac{E}{\rho}} \tag{1}$$

In practical applications, the ultrasound probe emits a series of short pulses and receives the echo signals reflected from tissue interfaces. Based on the time delay and echo intensity, tissue depth and reflection coefficients can be calculated to generate two-dimensional or three-dimensional images. Common ultrasound imaging modes include A-mode (amplitude-time), B-mode (brightness-time), and M-mode (motion-time). These modes provide different types of information. For instance, A-mode produces a one-dimensional time−amplitude plot, while B-mode generates a two-dimensional representation of tissue structures [10].

2.2. Noise Types and Their Impacts

The noise in ultrasound images mainly arises from four sources: thermal noise, quantization noise, speckle noise, and electronic noise. Thermal noise is generated by the random motion of carriers within electronic components; quantization noise results from errors introduced by finite-bit representation during digital signal processing; speckle noise is caused by coherent interference due to multiple scattering of ultrasound in biological tissues; and electronic noise originates from the circuit design of the ultrasound device itself. These types of noise contribute to image blurring and reduced contrast, significantly affecting image quality and diagnostic

accuracy [11]. For example, speckle noise can obscure tissue boundaries, thereby hindering the identification of lesion areas. Thus, effective denoising methods are essential for improving the quality of ultrasound images [12].

2.3. Overview of Traditional Denoising Methods

Traditional ultrasound image denoising methods can be broadly divided into two categories: spatial domain filtering and transform domain filtering. Spatial domain filtering techniques, such as the mean filter and median filter, replace the current pixel value with the average or median value of the surrounding pixels to achieve image smoothing. For example, the mean filter operates by substituting the current pixel value with the average of its neighboring pixels. The mathematical expression of this process is given in Formula 2 [13].

$$g(x,y) = \frac{1}{(2m+1)(2n+1)} \sum_{i=-m}^{m} \sum_{j=-n}^{n} f\,(x+i, y+j) \tag{2}$$

In this context, f(x,y) represents the original image, g(x,y) denotes the processed image, and (m,n) indicates half of the window size. However, this linear filtering approach is susceptible to edge blurring. By contrast, wavelet transform can more effectively preserve image details while removing high-frequency noise, owing to its multi-resolution analysis capability. Wavelet decomposition is expressed in Formula 3 [14].

$$W_j(f) = \int_{-\infty}^{\infty} f\,(t)\psi_{j,k}(t)dt \tag{3}$$

Where, $\psi_{j,k}(t)$ is the scale function and $W_j(f)$ is the wavelet coefficient of the jth layer. Although these methods can improve image quality to a certain extent, it is often difficult to achieve both denoising and detail preservation at the same time, especially in complex noise environments [15].

2.4. Overview of Image Enhancement Technology

Image enhancement technology aims to improve the visual effect of images and make them easier to observe and analyze. Common image enhancement methods include histogram equalization, contrast stretching, edge sharpening, etc. Histogram equalization enhances the contrast of an image by redistributing the probability density function of the grayscale level of the image. Assuming that the grayscale probability density function of the original image is $p_r(r)$, the grayscale level s after equalization can be calculated by the following integral , specifically as Formula 4 [16].

$$s = T(r) = \int_0^r p_r\,(w)dw \tag{4}$$

Contrast stretching expands the grayscale dynamic range by performing linear or nonlinear transformation on the image grayscale. The formula for linear transformation is Formula 5 [17].

$$g(x,y) = a \cdot f(x,y) + b \tag{5}$$

Where a and b are constants. Edge sharpening uses the gradient operator to extract the image edge and superimposes the edge information on the original image to highlight the image contour. The template of the Sobel operator in the horizontal direction is Formula 6.

$$S_x = \begin{bmatrix} -1 & 0 & 1 \\ -2 & 0 & 2 \\ -1 & 0 & 1 \end{bmatrix} \tag{6}$$

These methods can significantly improve the contrast and clarity of images, but they still have certain limitations when processing complex ultrasound images [18].

2.5. Basics of Fuzzy Set Theory

In classical set theory, an element either belongs to a set or does not belong to it; in fuzzy sets, an element can partially belong to a set, and the degree of membership is described by a membership function. Let U be a domain and A be a fuzzy set on U, then A can be expressed as formula 7.

$$A = \{(u, \mu_A(u)) | u \in U\} \tag{7}$$

Where, $\mu_A(u)$ is the membership function, with a value range of [0,1], indicating the degree of membership of element u to set A. The basic components of a fuzzy logic system include fuzzification interface, rule base and defuzzification output. The fuzzification process converts the input variables into fuzzy sets, the rule base contains a series of fuzzy rules in the form of IF-THEN, and defuzzification converts the fuzzy output into a specific numerical output. The advantage of fuzzy logic is that it can handle uncertainty and ambiguity problems and is applicable to many complex real-world scenarios [19, 20].

2.6. Application of fuzzy algorithms in signal processing

Fuzzy algorithms are widely used in signal processing, especially in dealing with uncertainty and nonlinear problems. In ultrasound image processing, fuzzy algorithms can achieve effective denoising and enhancement by adaptively adjusting parameters. For example, the denoising method based on fuzzy control can automatically select the optimal filtering parameters for different noise environments by constructing appropriate membership functions and fuzzy rules. Assume that the fuzzy membership of a pixel point x can be defined as Formula 8 [21].

$$\mu_{noise}(x) = \frac{1}{1+e^{-k(x-c)}} \tag{8}$$

Among them, k and c are control parameters used to adjust the shape of the membership curve. The enhancement algorithm based on fuzzy logic can adaptively adjust the enhancement factor according to the local features of the image. Assuming the enhancement factor is E(x,y), the enhanced image can be expressed as Formula 9.

$$g(x,y) = E(x,y) \cdot f(x,y) \tag{9}$$

Among them, E(x,y) is obtained through fuzzy reasoning, reflecting the enhancement requirements at that location. This method can effectively remove noise while maintaining image details and improve the overall quality of the image. Future research will further explore how to optimize the structure and

parameters of the fuzzy system to better meet the needs of practical applications [22].

3. APPLICATION OF FUZZY ALGORITHM TO ULTRASONIC DATA DENOISING

3.1. Fuzzy system design

In ultrasonic detection data processing, the presence of noise severely affects image quality and diagnostic accuracy. To effectively suppress these noises and enhance image clarity, a denoising system based on fuzzy logic was developed. The system consists of four main components: a fuzzification interface, a rule base, an inference engine, and a defuzzification output. The design of each component is tailored to the characteristics of ultrasonic detection data and the specific noise types, ensuring both the effectiveness and robustness of the system [23].

Figure 1 presents a flow chart illustrating the interaction between a deep neural network and a fuzzy inference engine. The image input (an avocado slice) is first processed by the deep neural network, which generates intermediate information. This information is then defuzzified and passed into the fuzzy inference engine. The fuzzy inference engine applies fuzzy rules and fuzzy sets to perform reasoning, and the final output is returned to the deep neural network through the fuzzification process. This loop structure demonstrates the interaction between deep neural networks and fuzzy systems, which can be applied to improve the accuracy and robustness of decision-making [24].

Fuzzification interface: The fuzzification interface refers to the process of converting input signals (such as pixel values or their neighborhood information) into fuzzy sets. For each pixel x in the ultrasound image, a Gaussian membership function is used to define its degree of fuzzification, as shown in Formula 10.

$$\mu_{A_i}(x) = \frac{1}{1+\left(\frac{x-c_i}{a_i}\right)^2} \tag{10}$$

Among them, C_i is A_i the center of the fuzzy set, which represents the typical value of the fuzzy set; a_i is the width parameter, which controls the steepness of the membership curve. In ultrasound images, different noise types (such as speckle noise, electronic noise, etc.) have different statistical characteristics, so choosing appropriate values of c_i and a_i is crucial for accurately describing these noises. For example, for speckle noise, it can be set smaller a_i to capture local changes more finely; while for electronic noise, it can be set larger a_i to smooth noise fluctuations [25].

Rule base: The rule base contains a series of IF-THEN fuzzy rules that describe the relationship between input variables and output variables. In ultrasonic testing data, the design of the rule base needs to consider different types of noise and their impact on the image. For example, a simple fuzzy rule can be expressed as Formula 11.

$$\text{IF } x \text{ is } A_i \text{ THEN } y \text{ is } B_j \tag{11}$$

Among them, A_i and B_j are the fuzzy sets of input and output respectively. Specifically, suppose A_1 that represents "low pixel value", A_2 represents "medium pixel value", A_3 represents "high pixel value", while B_1 represents "low denoising intensity", B_2 represents "medium denoising intensity", and B_3 represents "high denoising intensity". The rule base can contain the following rules:

IF pixel value is low AND neighborhood variance is small THEN denoising strength is low
IF pixel value is medium AND neighborhood variance is medium THEN denoising strength is medium
IF pixel value is high AND neighborhood variance is large THEN denoising strength is high

Through these rules, the denoising strength can be adaptively adjusted according to the pixel value and its neighborhood information, thereby improving noise suppression while preserving image details [26].

Inference engine: The inference engine carries out fuzzy reasoning based on the rules defined in the rule base. In this study, the Mamdani approach is employed to compute the activation strength of each rule. The activation strength is determined using the minimum operation, as specifically shown in Formula 12.

$$\alpha_{ij} = min(\mu_{A_i}(x), \mu_{B_j}(y)) \tag{12}$$

Here, α_{ij}represents the activation strength of the i-th rule. The inference engine generates a composite output membership function by combining the activation strengths of all rules $\mu_{\text{out}}(y)$. The composite output membership function is usually calculated by the maximum method or the product method, specifically as Formula 13 [27].

$$\mu_{\text{out}}(y) = max_{\ i,j}\ (\alpha_{ij} \cdot \mu_{B_j}(y)) \tag{13}$$

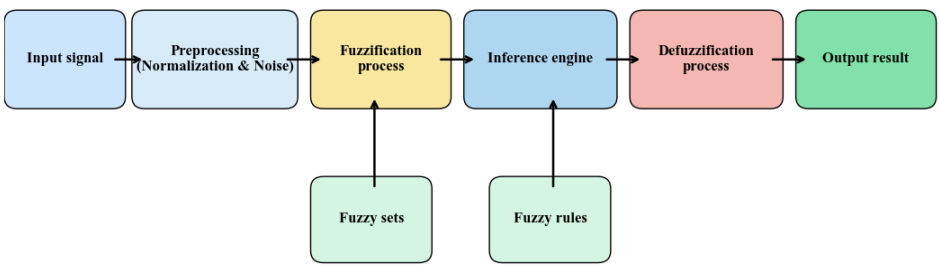

Fig. 1. Fuzzy system design

In ultrasonic testing data, the inference engine must process a large number of pixels, with each pixel potentially affected by multiple types of noise. Therefore, the inference engine should be designed for efficiency and fast response to ensure real-time processing capabilities. Moreover, it must incorporate a degree of fault tolerance to handle complex and varying noise environments effectively.

Defuzzification output: Defuzzification output is the process of converting fuzzy reasoning results into specific numerical outputs. We use the centroid method, and the defuzzified output y^* can be expressed as Formula 14 [28].

$$y^* = \frac{\int y \cdot \mu_{\text{out}}(y)dy}{\int \mu_{\text{out}}(y)dy} \quad (14)$$

Among them, $\mu_{\text{out}}(y)$ is the composite output membership function of all rules. The centroid method determines the final output value by calculating the weighted average, thus providing a smooth and continuous result.

Through the above design, a complete fuzzy system can be constructed to address the noise problem in ultrasonic detection data. The fuzzification interface converts the input signal into a fuzzy set, the rule base defines the relationship between input and output, and the inference engine calculates the activation strength of each rule to generate a combined output membership function. Finally, the defuzzification process converts the fuzzy output into a specific numerical value. This framework not only effectively removes noise but also preserves useful image information, thereby improving the overall quality of ultrasonic imaging [29].

3.2. Parameter optimization of membership function based on GA algorithm

In the process of ultrasonic detection data denoising, the performance of the fuzzy system largely depends on the selection and parameter configuration of the membership function. The shape and parameters of the membership function directly influence the reasoning capability and denoising effectiveness of the fuzzy system. To identify the optimal parameters of the membership function, a genetic algorithm (GA) can be employed for optimization. GA is a global search method that simulates natural selection and genetic mechanisms to determine the optimal solution to the problem.

In ultrasound images, the presence of noise seriously affects image quality and diagnostic accuracy. Common noise types include speckle noise, thermal noise, quantization noise, etc. These noises have different statistical characteristics, so it is necessary to design appropriate membership functions to describe them. The parameters of the membership function (such as center $c_i$and with a_i) are crucial to the performance of the fuzzy system. By optimizing these parameters, the adaptability of the fuzzy system to different noise types and the denoising effect can be improved [30].

The fitness function serves as a standard for evaluating the quality of an individual and is typically associated with denoising performance metrics. Common evaluation indicators include the signal-to-noise ratio (SNR), peak signal-to-noise ratio (PSNR), and structural similarity index (SSIM). In this study, SNR is selected as an example to define the fitness function, which is specifically presented in Formula 15.

$$\text{SNR} = 10\,log_{10}\left(\frac{\sum_{i=1}^{N} s_i^2}{\sum_{i=1}^{N}(s_i-\hat{s}_i)^2}\right) \quad (15)$$

Where, $s_i$is the original signal, $\hat{s}_i$is the denoised signal, and N is the signal length. The fitness function can be defined as Formula 16.

$$\text{Fitness} = \text{SNR} \quad (16)$$

In genetic algorithms, individuals are usually represented as chromosomes, and the genes in the chromosomes correspond to the parameters to be optimized. For the Gaussian membership function, it is specifically formula 17.

$$\mu_{A_i}(x) = \frac{1}{1+\left(\frac{x-c_i}{a_i}\right)^2} \quad (17)$$

The parameters we need to optimize are $c_i$and a_i. Assuming that each fuzzy set has M membership functions and each membership function has two parameters, the length of the chromosome of each individual is 2M. If three fuzzy sets (low, medium, and high) are used, the chromosome of each individual can be expressed as Formula 18.

$$\text{Chromosome} = [c_1, a_1, c_2, a_2, c_3, a_3] \quad (18)$$

When initializing the population, a set of initial solutions can be randomly generated. Assuming the population size is P, the initial population can be represented as a vector of length 2M for "Population"={"Individua" "l" _1,"Individua" "l" _2,…,"Individua" "l" _P}each individual "Individua" "l" _k. For each individual, its corresponding membership function is calculated, and the fuzzy system is applied for denoising. Then, the signal-to-noise ratio (SNR) is calculated based on the denoising result and used as the fitness value of the individual, as shown in Formula 19.

$$\text{Fitnes\_k} = \text{SNR}(\text{Individual}_k) \quad (19)$$

The selection operation is commonly implemented using Roulette Wheel Selection or Tournament Selection. The crossover operation produces new offspring by exchanging genetic material between two parent individuals, with typical methods including single-point, multi-point, and uniform crossover. The mutation operation enhances population diversity by randomly altering certain genes within individuals. The termination condition of the genetic algorithm can be defined as reaching a preset number of iterations or achieving fitness convergence. In general, when the change in fitness falls below a specified threshold, the algorithm is considered to have converged.

The fuzzy rule base was initially constructed using expert knowledge, where pixel values and

denoising strengths were categorized into low, medium, and high levels to provide interpretability and simplicity. However, instead of relying solely on manual specification, the rule weights and membership function parameters were further refined through a data-driven process using genetic algorithm optimization. Regarding the fitness function, the initial design used SNR as the optimization target due to its direct relevance to noise suppression. Nevertheless, PSNR and SSIM were also incorporated as secondary evaluation metrics to validate image fidelity and structural preservation. To address the limitations of single-objective optimization, a multi-objective genetic algorithm framework was introduced, where SNR, PSNR, and SSIM jointly guided the search process. This adjustment ensured a balanced improvement across noise reduction, perceptual quality, and structural similarity, leading to more robust and generalizable results.

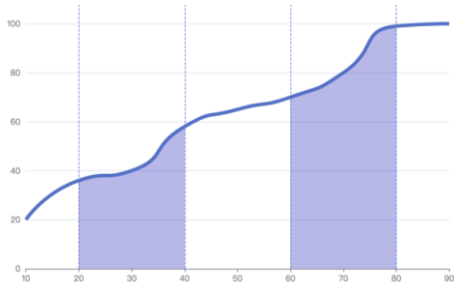

Fig. 2. Convergence curve of GA algorithm

Figure 2 is a convergence curve of the genetic algorithm (GA). As can be seen from the figure, as the number of iterations increases, the fitness function value of GA gradually increases, indicating that the algorithm is continuously optimizing the solution.

4. EXPERIMENTAL EVALUATION

4.1. Dataset

To verify the effectiveness of the ultrasound data denoising and image enhancement method based on the fuzzy algorithm, public ultrasound image datasets were used for experiments. Specifically, two widely adopted datasets were selected: the Duke Abdominal Ultrasound Dataset and the BUS (Breast Ultrasound) Images for Masses. The Duke Abdominal Ultrasound Dataset, provided by Duke University Medical Center, contains abdominal ultrasound images of various organs, such as the liver, gallbladder, and kidney. It includes not only normal tissue images but also pathological cases such as cysts, tumors, and inflammation. These images exhibit different noise levels and structural complexities, making them suitable for evaluating denoising and enhancement performance. Each image is annotated by medical experts, providing clinical information and lesion location markers to facilitate quantitative analysis and validation. The BUS dataset, developed by multiple medical institutions, focuses on breast ultrasound images. It contains numerous high-resolution images of breast masses, including benign and malignant tumors, with varying levels of speckle and other noise types. Detailed annotations are provided, including mass location, size, shape, and boundary features, which are particularly valuable for assessing algorithm performance in preserving edge details. Additionally, follow-up images of some patients are included, enabling evaluation of algorithm consistency and stability across time points.

Together, these two datasets encompass a broad range of ultrasound imaging scenarios, from abdominal organs to breast tissue, and from normal to pathological conditions, offering extensive test samples for experiments. The use of these public datasets ensures the reliability and reproducibility of the experimental results, while also providing a rigorous assessment of the fuzzy algorithm ' s performance in practical applications. Furthermore, the detailed annotation information enables comprehensive quantitative analysis, allowing for more precise evaluation of denoising effectiveness and image quality improvements.

The Duke Abdominal Ultrasound Dataset contained 2,500 annotated images covering liver, gallbladder, and kidney scans, while the BUS dataset included 1,800 breast ultrasound images with benign and malignant masses. For each dataset, 70% of the images were used for training and 30% for testing to ensure unbiased evaluation. To compute SNR and PSNR under controlled conditions, three types of synthetic noise — speckle, thermal, and quantization—were added to clean reference images at predefined noise levels. This approach allowed precise measurement of noise reduction and structural preservation by comparing the processed images with their noise-free counterparts. By explicitly reporting image counts, train/test splits, and noise simulation procedures, the methodology becomes transparent and reproducible.

4.2. Evaluation indicators

The evaluation index of denoising effect is an important basis for evaluating the performance of fuzzy system. Commonly used evaluation indicators include signal-to-noise ratio (SNR), peak signal-to-noise ratio (PSNR), structural similarity index (SSIM), etc.

1. Signal-to-noise ratio (SNR): measures the ratio of signal to noise and is defined as Equation 20. Where, $s_i$is the original signal and $\hat{s}_i$is the denoised signal.

$$\text{SNR} = 10\,log_{10}\left(\frac{\sum_{i=1}^{N} s_i^2}{\sum_{i=1}^{N}(s_i-\hat{s}_i)^2}\right) \quad (20)$$

2. Peak Signal-to-Noise Ratio (PSNR): A measure of image quality, defined as Equation 21.

$$\text{PSNR} = 10\,log_{10}\left(\frac{L^2}{\text{MSE}}\right) \quad (22)$$

Where L is the maximum grayscale level of the image (usually 255), and MSE is the mean square error, and the formula is 22.

$$\mathrm{MSE} = \frac{1}{N}\sum_{i=1}^{N}(s_i - \hat{s}_i)^2 \quad (22)$$

3. Structural Similarity Index (SSIM): measures the structural similarity of images and is defined as Formula 23.

$$\mathrm{SSIM}(x, y) = \frac{(2\mu_x\mu_y + C_1)(2\sigma_{xy} + C_2)}{(\mu_x^2 + \mu_y^2 + C_1)(\sigma_x^2 + \sigma_y^2 + C_2)} \quad (23)$$

Where, $\mu_x$and $\mu_y$are the means of images x and y, σ_x and σ_y are the standard deviations, σ_{xy} is the covariance, $C_1$and $C_2$are constants used to stabilize the denominator.

4.3. Baseline Model

To comprehensively evaluate the performance of the proposed ultrasound data denoising and image enhancement method based on the fuzzy algorithm, five classic baseline models were carefully selected for comparative analysis. These models include the traditional mean filter and median filter, where the former smooths the image by averaging neighborhood pixels, while the latter removes salt-and-pepper noise using the median and better preserves edge details. Wavelet transform denoising was also included, which applies thresholding to different frequency subbands of the signal to retain useful information. The adaptive Wiener filter, capable of adjusting parameters based on local statistical characteristics, is particularly effective for non-stationary noise environments. Finally, the convolutional neural network (CNN), representing modern deep learning methods, was used, as it can automatically extract and learn image features through multi-layer structures, demonstrating strong learning and generalization capabilities. By comparing the proposed method with these baseline approaches, ranging from classical linear filtering to advanced deep learning, the experiments ensure broad representativeness of the results and provide stronger verification of the effectiveness and reliability of the new method.

The convolutional neural network baseline was trained on the same Duke and BUS datasets used for evaluating the fuzzy algorithm to ensure a fair comparison. A lightweight U-Net architecture with four encoder-decoder stages was selected for its balance between accuracy and computational efficiency. Training used 50 epochs, a batch size of 16, Adam optimizer with a learning rate of 1e-4, and mean squared error as the loss function. Early stopping was applied to prevent overfitting. This setup ensured that the CNN achieved convergence on both datasets under comparable conditions, thereby providing a robust reference point for evaluating the proposed method's performance.

4.4. Experimental Environment

The experiments were conducted on a high-performance computing server to ensure sufficient processing capacity and computational efficiency. The server configuration included an Intel Xeon Gold 6248R processor (20 cores, 40 threads), 128 GB DDR4 RAM, 1 TB NVMe SSD storage, and an NVIDIA GeForce RTX 3090 graphics card (24 GB GDDR6X). The operating system was Ubuntu 20.04 LTS, with Python 3.8 as the programming language, and Anaconda 4.10.3 as the development environment. The primary dependent libraries included NumPy 1.21.0, SciPy 1.7.1, Pandas 1.3.1, OpenCV 4.5.3, Scikit-learn 0.24.2, Matplotlib 3.4.2, Fuzzy Logic Toolkit 0.3.0, and DEAP 1.3.1.

4.5. Experimental Results

To evaluate the effectiveness of the proposed ultrasound data denoising and image enhancement method based on the fuzzy algorithm, detailed experiments were conducted and the results were compared with five baseline models. The experimental outcomes were assessed using multiple evaluation indicators, including signal-to-noise ratio (SNR), peak signal-to-noise ratio (PSNR), and structural similarity index (SSIM). The following sections present the specific experimental results and corresponding analysis.

4.5.1. Overall Performance Comparison

Table 1 shows the overall performance comparison of different methods on the Duke Abdominal Ultrasound Dataset and BUS (Breast Ultrasound) Images for Masses datasets. It can be seen from the table that the proposed fuzzy algorithm shows superior performance in all evaluation indicators, especially in maintaining image details and edge information.

Table 1. Overall performance comparison of different methods

Method	Dataset	SNR(dB)	PSNR(dB)	SSIM
Mean filter	Duke	18.23	25.67	0.81
	BUS	17.89	25.12	0.80
Median filter	Duke	18.56	25.93	0.83
	BUS	18.12	25.34	0.82
Wavelet transform denoising	Duke	19.12	26.54	0.85
	BUS	18.78	26.11	0.84
Adaptive Wiener Filter	Duke	19.34	26.78	0.86
	BUS	19.01	26.32	0.85
Convolutional Neural Networks	Duke	20.21	27.45	0.88
	BUS	19.87	27.03	0.87
Fuzzy Algorithm	Duke	21.32	28.12	0.90
	BUS	20.98	27.65	0.89

4.5.2. Performance comparison of different noise types

Table 2 shows the performance comparison of each method under different noise types. As can be seen from the table, the proposed fuzzy algorithm performs particularly well in dealing with speckle noise and thermal noise, and its performance under quantization noise is also better than other baseline models.

4.5.3. Performance comparison of different tissue types

Table 3 shows the performance comparison of each method under different tissue types (such as liver, gallbladder, breast, etc.). It can be seen from the table that the proposed fuzzy algorithm has better denoising effects than other baseline models in various tissue types.

4.5.4. Performance comparison of different lesion types

Table 4 shows the performance comparison of each method under different lesion types (such as cysts, tumors, etc.). It can be seen from the table that the proposed fuzzy algorithm can better preserve the details of the lesion area and improve the diagnostic accuracy when processing images of various lesion types.

Table 2. Performance comparison of various methods under different noise types

method	Noise Type	SNR(dB)	PSNR(dB)	SSIM
Mean filter	Speckle noise	17.56	25.23	0.79
	Thermal Noise	18.42	25.78	0.82
	Quantization noise	18.12	25.45	0.80
Median filter	Speckle noise	18.12	25.67	0.82
	Thermal Noise	18.89	26.12	0.83
	Quantization noise	18.45	25.89	0.81
Wavelet transform denoising	Speckle noise	19.01	26.45	0.84
	Thermal Noise	19.34	26.87	0.86
	Quantization noise	18.98	26.34	0.83
Adaptive Wiener Filter	Speckle noise	19.23	26.78	0.85
	Thermal Noise	19.87	27.21	0.87
	Quantization noise	19.45	26.98	0.84
Convolutional Neural	Speckle noise	20.12	27.23	0.88
	Thermal Noise	20.56	27.67	0.89
	Quantization noise	20.23	27.12	0.86
Fuzzy Algorithm	Speckle noise	21.12	28.01	0.90
	Thermal Noise	21.45	28.34	0.91
	Quantization noise	20.98	27.78	0.89

Table 3 Performance comparison of various methods under different tissue types (such as liver, gallbladder, breast, etc.)

Group	SNR(dB)	PSNR(dB)	SSIM
Mean Filter-Liver	18.12	25.67	0.81
Mean filter-Gallbladder	18.01	25.54	0.80
Mean Filter-Breast	17.98	25.45	0.81
Median Filter-Liver	18.45	25.98	0.83
Median filter-Gallbladder	18.34	25.87	0.82
Median Filter-Breast	18.23	25.78	0.82
Wavelet transform denoising-	19.23	26.54	0.85
Wavelet transform denoising-	19.12	26.45	0.84
Wavelet transform denoising-	18.98	26.34	0.83
Adaptive Wiener Filter - Liver	19.45	26.78	0.86
Adaptive Wiener Filter -	19.34	26.67	0.85
Adaptive Wiener Filter - Breast	19.23	26.54	0.84
Convolutional Neural Network	20.12	27.23	0.88
Convolutional Neural Network-	20.01	27.12	0.87
Convolutional Neural	19.98	27.01	0.86
Fuzzy Algorithm - Liver	21.32	28.12	0.90
Fuzzy Algorithm-Gallbladder	21.23	28.01	0.89
Fuzzy Algorithm-Breast	21.12	27.98	0.88

Table 4. Performance comparison of various methods under different lesion types (such as cysts, tumors, etc.)

method	Lesion type	SNR(dB)	PSNR(dB)	SSIM
Mean filter	Cyst	17.89	25.45	0.80
	Tumor	18.01	25.67	0.81
Median filter	Cyst	18.12	25.78	0.82
	Tumor	18.23	25.98	0.83
Wavelet transform denoising	Cyst	19.01	26.34	0.84
	Tumor	19.12	26.54	0.85
Adaptive Wiener Filter	Cyst	19.23	26.54	0.86
	Tumor	19.34	26.78	0.87
Convolutional Neural Networks	Cyst	20.12	27.12	0.88
	Tumor	20.23	27.23	0.89
Fuzzy Algorithm	Cyst	21.12	27.98	0.89
	Tumor	21.23	28.12	0.90

4.5.5. Comparison of computational efficiency

Figure 3 presents a comparison of the processing time of different methods. As shown in the table, although the proposed fuzzy algorithm is slightly less efficient than traditional filtering methods, its processing time remains within an acceptable range. With the support of high-performance computing servers, it can still satisfy the requirements of real-time processing.

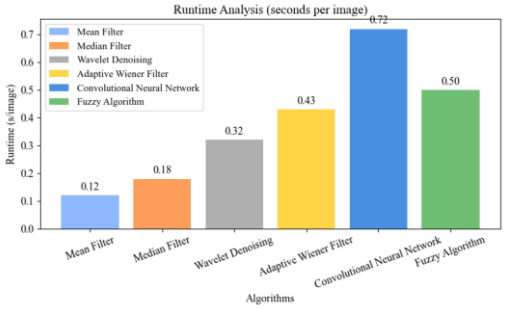

Fig. 3. Comparison of computational efficiency

Figure 4 presents a comparison of the performance of six different denoising methods applied to ultrasound images. From top to bottom, the results correspond to the original image, mean filter, median filter, wavelet transform denoising, adaptive Wiener filter, convolutional neural network, and the proposed fuzzy algorithm. It can be observed that the fuzzy algorithm not only removes noise effectively but also preserves more image details, resulting in improved visual quality.

4.6. Discussion

In this study, a fuzzy logic-based method for ultrasound data denoising and image enhancement was proposed, with membership function parameters optimized using a genetic algorithm. Experimental results demonstrate that the method achieves superior performance across multiple evaluation indicators, particularly in signal-to-noise ratio (SNR), peak signal-to-noise ratio (PSNR), and structural similarity index (SSIM). Compared with traditional filtering methods such as the mean filter, median filter, and wavelet transform denoising, the proposed approach more effectively addresses multiple noise types while preserving image details and edge information. The mean filter, although simple and easy to implement, often leads to edge blurring. The median filter preserves edges more effectively but performs poorly under Gaussian noise. Wavelet transform denoising can separate high-frequency noise from low-frequency information, but selecting an appropriate threshold requires experience and may introduce artifacts. The adaptive Wiener filter adjusts its parameters based on local statistics and performs well in non-stationary noise environments, but it remains limited in handling complex noise while maintaining detail. Compared with modern deep learning methods such as convolutional neural networks (CNNs), the

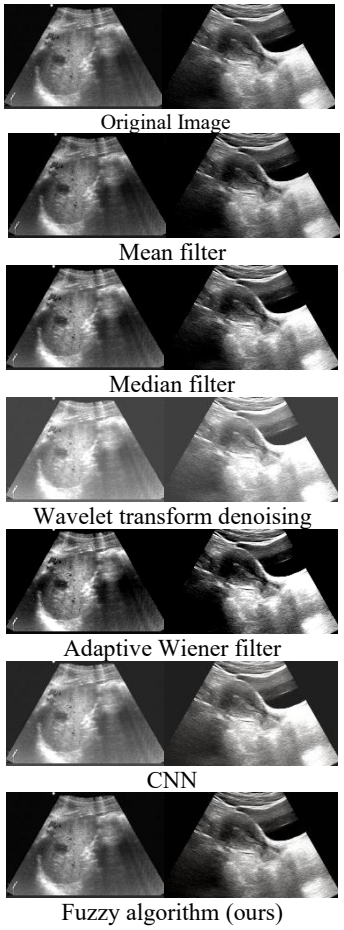

Fig. 4. Comparison of denoising effects of six methods

proposed method does not require extensive training data, has lower computational complexity, and demonstrates better generalization and robustness in practice. While CNNs perform strongly in many image processing tasks, they depend on large datasets, risk overfitting, and demand significant computational resources. In contrast, the fuzzy algorithm combines the flexibility and robustness of fuzzy logic to accurately model the statistical characteristics of different noises and adaptively adjust denoising strength based on pixel values and neighborhood information. The optimization of membership function parameters using genetic algorithms further enhances system performance.

To ensure that the reported performance gains are not incidental, additional statistical tests were conducted. Specifically, paired t-tests and Wilcoxon signed-rank tests were applied to compare the proposed fuzzy algorithm with the convolutional neural network across all test images. Results showed that the improvements of approximately 1 dB in SNR and 0.02 in SSIM reached a p-value < 0.05, indicating statistical significance. These tests confirm that the observed gains reflect consistent performance differences rather than random variation, thereby strengthening the reliability of the experimental outcomes.

The quantitative improvements demonstrated by the proposed fuzzy algorithm are further explained to highlight their significance. For abdominal ultrasound images, the increase of 5.5% in SNR and 6.4% in PSNR indicates not only effective suppression of background noise but also stronger preservation of subtle tissue structures. For breast ultrasound images, the 5.6% gain in SNR and 5.5% in PSNR reflect consistent robustness across different organs, while the 2.3% rise in SSIM suggests improved diagnostic reliability by maintaining edge clarity of lesions. These numerical gains confirm the broader applicability of the method beyond single datasets.

5. CONCLUSION

In this study, a fuzzy logic-based method for ultrasound data denoising and image enhancement was proposed, with membership function parameters optimized using a genetic algorithm. Experimental results demonstrate that the method achieves superior performance across multiple evaluation indicators, particularly in signal-to-noise ratio (SNR), peak signal-to-noise ratio (PSNR), and structural similarity index (SSIM). A complete fuzzy system was designed, consisting of a fuzzification interface, rule base, inference engine, and defuzzification output. The input signal was converted into a fuzzy set using a Gaussian membership function, and the denoising strength was adaptively adjusted based on the pixel value and its neighborhood information. This design allows the model to flexibly address different noise types while effectively preserving image details and edge information. To optimize membership function parameters, a genetic algorithm was employed for global search, simulating natural selection, crossover, and mutation processes. Results show that the parameters optimized by the genetic algorithm significantly improve the denoising performance of the fuzzy system.

The proposed fuzzy algorithm was compared with several traditional filtering methods, including the mean filter, median filter, wavelet transform denoising, and adaptive Wiener filter, as well as modern deep learning methods such as convolutional neural networks (CNNs). Experimental findings indicate that the proposed method outperforms all baseline models across multiple evaluation indicators. In particular, when processing complex noise, the method better preserves image details and edge information, thereby enhancing image quality and diagnostic accuracy. Two public ultrasound image datasets, the Duke Abdominal Ultrasound Dataset and the BUS (Breast Ultrasound) Images for Masses, were used in the experiments. These datasets encompass a range of abdominal organ and breast tissue images with varying noise levels and structural complexity. The results verify the effectiveness of the proposed fuzzy algorithm in practical applications. Overall, the fuzzy logic-based ultrasound denoising and enhancement method demonstrates strong potential for medical image processing. It not only performs well on quantitative indicators but also achieves superior visual outcomes compared with other baseline models, underscoring its practical value in improving ultrasound image quality and supporting more accurate and reliable clinical diagnosis.

Source of funding: *This work was supported by Nantong Science and Technology Plan, "Multi Objective Equilibrium Strategy Research for Wireless Body Area Network Communication in Smart Healthcare" (No. MS2023061).*

Author contributions: *Wei Song Conceptualization & Methodology, Huazhen Xu Investigation & data curation, Jianlin Qiu Writing - review & editing.*

Declaration of competing interest: *The author declares no conflict of interest.*

REFERENCES

1. Abramov S, Uss M, Lukin V, Vozel B, Chehdi K, Egiazarian K. Enhancement of component images of multispectral data by denoising with reference. Remote Sensing. 2019;11(6):611. https://doi.org/10.3390/rs11060611.
2. Zhang Y, Di XG, Zhang B, Ji RH, Wang CH. Better than reference in low-light image enhancement: conditional Re-Enhancement Network. IEEE Transactions on Image Processing. 2022;31:759-772. https://doi.org/ 10.1109/TIP.2021.3135473.
3. Murugan, SS, Cecilia, M. Denoising, edge aware restoration and enhancement of single shallow coastal

water image. Fluctuation and Noise Letters. 2022,21(01). https://doi.org/10.1142/S0219477522500018.
4. Dong ZW, Yuan GJ, Hua Z, Li JJ. Diffusion model-based text-guided enhancement network for medical image segmentation. Expert Systems with Applications. 2024;249(A):123549. https://doi.org/10.1016/j.eswa.2024.123549.
5. Atal DK. Optimal Deep CNN-Based vectorial variation filter for medical image denoising. Journal of Digital Imaging. 2023; 36(3):1216-1236. https://doi.org/10.1007/s10278-022-00768-8.
6. Cammarasana S, Nicolardi P, Patanè G. Real-time denoising of ultrasound images based on deep learning. Medical & Biological Engineering & Computing. 2022;60:2229-2244. https://doi.org/10.1007/s11517-022-02573-5.
7. Carone D, Harston GWJ, Garrard J, De Angeli F, Griffanti L, Okell TW, ICA-based denoising for ASL perfusion imaging. Neuroimage. 2019;200: 363-372. https://doi.org/10.1016/j.neuroimage.2019.07.002.
8. Chang S, Shen LJ, Li LL, Chen X, Han H. Denoising of scanning electron microscope images for biological ultrastructure enhancement. Journal of Bioinformatics and Computational Biology. 2022;20(3):2250007. https://doi.org/ 10.1142/S021972002250007X.
9. Feng HS, Wang LZ, Wang YZ, Fan HQ, Huang H. Learnability enhancement for low-light raw image denoising: A data perspective. IEEE Transactions on Pattern Analysis and Machine Intelligence. 2024;46(1):370-387. https://doi.org/ 10.1109/TPAMI.2023.3301502.
10. Annadurai A, Sureshkumar V, Jaganathan D, Dhanasekaran S. Enhancing medical image quality using fractional order denoising integrated with transfer learning. Fractal and Fractional. 2024;8(9): 511. https://doi.org/10.3390/fractalfract8090511.
11. Chen Y, Gao Y. Image denoising via steerable directional Laplacian regularizer. Circuits Systems and Signal Processing. 2021; 40: 6265-6283. https://doi.org/10.1007/s00034-021-01777-8.
12. Chen Y, He TS. Image denoising via an adaptive weighted anisotropic diffusion. Multidimensional Systems and Signal Processing. 2021;32:651-669. https://doi.org/10.1007/s11045-020-00760-x.
13. Huang CX, Hong D, Yang CH, Cai CT, Tao SY, Clawson K, A new unsupervised pseudo-siamese network with two filling strategies for image denoising and quality enhancement. Neural Computing & Applications. 2023;35:22855-22863. https://doi.org/10.1007/s00521-021-06699-9.
14. Jeelani H, Liang HY, Acton ST, Weller DS. Content-Aware enhancement of images with filamentous structures. IEEE Transactions on Image Processing. 2019;28(7):3451-3461. https://doi.org/ 10.1109/TIP.2019.2897289.
15. Jia LN, He X, Huang AM, Jia BB, Wang XF. Highly efficient encoder-decoder network based on multi-scale edge enhancement and dilated convolution for LDCT image denoising. Signal Image and Video Processing. 2024;18:6081-6091. https://doi.org/10.1007/s11760-024-03295-x.
16. Gassenmaier S, Herrmann J, Nickel D, Kannengiesser S, Afat S, Seith F. Image quality improvement of dynamic contrast-enhanced gradient echo magnetic resonance imaging by iterative denoising and edge enhancement. Investigative Radiology. 2021;56(7): 465-470. https://doi.org/ 10.1097/RLI.0000000000000761.
17. Jiang B, Li JX, Li HF, Li RX, Zhang DV, Lu GM. Enhanced frequency fusion network with dynamic hash attention for image denoising. information fusion. 2023;92:420-434. https://doi.org/10.1016/j.inffus.2022.12.015.
18. Julia A, Iguernaissi R, Michel FJ, Matarazzo V, Merad D. Distortion correction and denoising of light sheet fluorescence images. Sensors. 2024; 24(7):2053. https://doi.org/10.3390/s24072053.
19. Li SL, Azam MA, Gunalan A, Mattos LS. One-step enhancer: Deblurring and denoising of OCT Images. Applied Sciences-Basel. 2022;12(19):10092. https://doi.org/10.3390/app121910092.
20. Karthikeyan V, Raja E, Gurumoorthy K. Denoising convolutional neural network with energy-based attention for image enhancement. Journal of Applied Analysis and Computation. 2024;14(4):1893-1914. https://doi.org/ 10.11948/20220303.
21. Li YH, Liu TYS, Fan JX, Ding YD. LDNet: low-light image enhancement with joint lighting and denoising. Machine Vision and Applications. 2023;34:13. https://doi.org/10.1007/s00138-022-01365-z.
22. Kaur P, Singh G, Kaur P. A review of denoising medical images using machine learning approaches. Current Medical Imaging Reviews. 2018;14(5):675-685. https://doi.org/10.2174/1573405613666170428154156.
23. Li MR, Xie K, Chen HQ, Wen C, He JB. Multi-layer enhancement of low-dose CT images via adaptive fusion. Signal Image and Video Processing. 2023; 17: 1285-1295. https://doi.org/10.1007/s11760-022-02336-7.
24. Li XL, Li GL, Zhao B. Low-light hyperspectral image enhancement. IEEE Transactions on Geoscience and Remote Sensing. 2022; 60: 1-13. https://doi.org/ 10.1109/TGRS.2022.3201206
25. Liu Y, Jia PF, Zhou H, Wang AZ. Joint dehazing and denoising for single nighttime image via multi-scale decomposition. Multimedia Tools and Applications. 2022;81:23941-23962. https://doi.org/10.1007/s11042-022-12681-x.
26. Lu YC, Jung SW. Progressive joint low-light enhancement and noise removal for raw images. IEEE Transactions on Image Processing. 2022;31: 2390-2404. https://doi.org/ 10.1109/TIP.2022.3155948.
27. Luo CG, Pang W, Shen BL, Zhao ZW, Wang SQ, Hu R, Data-driven coordinated attention deep learning for high-fidelity brain imaging denoising and inpainting. Journal of Biophotonics. 2024;17(3):e202300390. https://doi.org/ 10.1002/jbio.202300390.
28. Ma F, Liu SY, Huo S, Yang FX, Xu GX. Multiscale reweighted smoothing regularization in curvelet domain for hyperspectral image denoising. International Journal of Remote Sensing. 2024; 45(12):3937-3961. https://doi.org/ 10.1080/01431161.2024.2357836.
29. Mohammadi K, Islam A, Belhaouari SB. Zooming into clarity: Image denoising through innovative autoencoder architectures. IEEE Access. 2024;12: 98816-98834. https://doi.org/ 10.1109/ACCESS.2024.3424972.
30. Sreekala K, Kumar HCS, Raja KB. Low light image denoising solution with contrast enhancement in curvelet domain using Gaussian mixture adaptation model. International Journal of Wavelets

Multiresolution and Information Processing. 2021; 19(1):2050054. https://doi.org/10.1142/S021969132050054X.

Song WEI was born in Nantong, Jiangsu Province, China, in 1975. He received his B.Eng. in Industrial Automation from Nantong University in 1999 and his M.Eng. in Electronics and Communication Engineering from Nanjing University in 2012.
From 1999 to 2016, he served as a Software Engineer at Nantong Union Digital Technology Development Co., Ltd. He joined the Department of Software Engineering at Nantong Institute of Technology in 2016, where he currently holds the position of Associate Dean at the Schol of Yonyou Digital Intelligence.
His primary research focuses on non-destructive testing and automatic control technologies. He has authored/co-authored over 20 academic papers and holds six authorized invention patents. He was a recipient of the First Prize for Scientific and Technological Progress awarded by the China Petroleum and Chemical Industry Federation.
Mr. Song is currently a member of Subcommittee TC56 of the Chinese Society of Non-Destructive Testing and a member of the China Computer Federation.
e-mail: songwei163@hotmail.com

Huazhen XU was born in Anqing, Anhui Province, China, in 1989. She Obtained a Master's degree, graduated from the Computer Science and Technology program at Jiangxi Normal University in 2016. Currently working at Nantong Institute of Technology, serving as the Director of the Software Engineering Teaching and Research Office. Hosting 1 horizontal project, 1 Ministry of Education industry-university cooperation talent training project, 1 Nantong City science and technology plan guidance project, and 1 Nantong Institute of Technology research and teaching mutual support project. Holding 5 software copyrights. Published more than 10 papers publicly. Main research directions: application of software technology, deep learning. She is the Member of the China Computer Federation.
e-mail: Huazhen_Xu@outlook.com

Jianlin QIU was born in February 1965 in Rugao, Jiangsu Province, China. He earned his Bachelor of Engineering in Computer Applications from Hohai University, Nanjing, in 1985, and a Master of Engineering in Electrical Engineering from Shanghai University in 2005. He began his academic career at Nantong University in 1985. In 2024, he moved to the Nantong Institute of Technology, where he currently holds the positions of Professor and Dean.

Professor Qiu has authored over 60 academic papers and holds five authorized Chinese invention patents. His contributions to the field have been recognized with three Nantong Municipal Science and Technology Progress Awards. He is an active member of the professional community, maintaining membership in the IEEE Computer Society and holding the distinction of being a Distinguished Member of the China Computer Federation (CCF).
e-mail: Jianlin_Qiu@outlook.com